Dev Genes Evol (2016) 226:413–422
DOI 10.1007/s00427-016-0562-3

ORIGINAL ARTICLE

Observations on germ band development in the cellar spider *Pholcus phalangioides*

Natascha Turetzek[1,2] · **Nikola-Michael Prpic**[1,2]

Received: 19 April 2016 / Accepted: 22 August 2016 / Published online: 1 September 2016

Abstract Most recent studies of spider embryonic development have focused on representatives of the species-rich group of entelegyne spiders (over 80 % of all extant species). Embryogenesis in the smaller spider groups, however, is less well studied. Here, we describe the development of the germ band in the spider species *Pholcus phalangioides*, a representative of the haplogyne spiders that are phylogenetically the sister group of the entelegyne spiders. We show that the transition from radially symmetric embryonic anlage to the bilaterally symmetric germ band involves the accumulation of cells in the centre of the embryonic anlage (primary thickening). These cells then disperse all across the embryonic anlage. A secondary thickening of cells then appears in the centre of the embryonic anlage, and this thickening expands and forms the segment addition zone. We also confirm that the major part of the opisthosoma initially develops as a tube shaped structure, and its segments are then sequentially folded down on the yolk during inversion. This special mode of opisthosoma formation has not been reported for entelegyne spiders, but a more comprehensive sampling of this diverse group is necessary to decide whether this peculiarity is indeed lacking in the entelegyne spiders.

Keywords Embryonic development · Haplogyne spiders · *Pholcus phalangioides* · Opisthosoma · Leg length · *Engrailed*

Communicated by Angelika Stollewerk

Electronic supplementary material The online version of this article (doi:10.1007/s00427-016-0562-3) contains supplementary material, which is available to authorized users.

✉ Nikola-Michael Prpic
nprpic@uni-goettingen.de

[1] Johann-Friedrich-Blumenbach-Institut für Zoologie und Anthropologie, Georg-August-Universität Göttingen, Abteilung für Entwicklungsbiologie, 37077 Göttingen, Germany

[2] Göttingen Center for Molecular Biosciences (GZMB), Ernst-Caspari-Haus, Justus-von-Liebig-Weg 11, 37077 Göttingen, Germany

Introduction

Spider development involves, after cleavage and blastoderm formation, the formation of a disc-shaped embryonic anlage (that represents the embryo proper) and a significant portion of extra embryonic cells. In some species, including the model species *Cupiennius salei* (Wolff and Hilbrant 2011) and *Pholcus phalangioides* (the species studied here), the morphology of cells in the embryonic anlage and in the extra embryonic region is very similar and a clear border is difficult to discern. In other species like in the two model species *Latrodectus mactans* and *Parasteatoda tepidariorum* (formerly placed in the genus *Achaearanea*), the extra embryonic cells are yolk-rich and are significantly larger than the cells in the embryonic anlage (Mittmann and Wolff 2012; Edgar et al. 2015). In these cases, when the embryonic anlage is morphologically well-separated from the extra embryonic portion, the embryonic anlage is called a "germ-disc." The embryonic anlage is radially symmetric and therefore needs to undergo a transition from radial to bilateral symmetry to form the germ band and ultimately the bilaterally symmetric spider. This process of symmetry break at the transition from embryonic anlage to germ band involves the migration of a group of cells, called the cumulus, from the centre to the perimeter of the disc-shaped embryonic anlage. Several genes that are required for cumulus migration have been identified in the spider species *P. tepidariorum* (Akiyama-Oda and Oda

2003, 2006, 2010), but the mechanisms of symmetry break are still not fully understood.

The majority of molecular studies of spider development focused on entelegyne spiders (e.g., Abzhanov and Kaufman 2000; Akiyama-Oda and Oda 2003; McGregor et al. 2008). Although this group of spiders includes the vast majority of all spider species (ca. 33,000 species (i.e., over 80 %)), it is unclear whether the processes described on the basis of entelegyne spiders are also representative of the other, smaller spider groups. We have therefore initiated comparative studies in the haplogyne spiders which are phylogenetically the sister group of the entelegyne spiders, but comprise only about 3500 species worldwide. We have chosen the species *Pholcus phalangioides* as a very common and therefore easily accessible species. The majority of the species of the genus *Pholcus* are distributed in Asia, but a few species also have a western Palaearctic distribution, and *P. phalangioides* is even a cosmopolitan species (Huber 2011). The species of *Pholcus* are characterised by their extremely long walking legs that make the animals superficially similar to long-legged species of harvestmen and that have earned them their nickname "daddy long leg spiders." So far, we have studied patterning functions in appendage development in *P. phalangioides* (Pechmann et al. 2011; Turetzek et al. 2016). Here, we focus on the description of germ band formation and the further differentiation of the germ band.

Materials and methods

Pholcus phalangioides husbandry and embryo fixation

Our *P. phalangioides* husbandry is kept at controlled temperature (25 °C) and dark/light cycle (10 h of light). The animals are kept separate in plastic vials sealed with styrene foam plugs and are supplied regularly with water and food. Juveniles are fed with *Drosophila melanogaster* flies, older stages and adults are fed with larger flies (*Musca domestica* and *Lucilia caesar*) or juvenile crickets (*Acheta domesticus*). After mating, several cocoons are produced by the females at irregular intervals, each cocoon containing between 50 and 100 eggs. Freshly made cocoons were removed from the females with forceps after anaesthesia with carbon dioxide and kept separately in glass test tubes until the eggs were removed for fixation. Fixation of *P. phalangioides* embryos was performed according to the fixation protocol previously published for *C. salei* (Prpic et al. 2008a).

Gene cloning

cDNA was synthesised with the SMARTer™ RACE kit (Clontech Laboratories) from total RNA of mixed embryonic stages prepared with TRIzol® (Invitrogen) according to the manufacturer's instructions. Initial fragments of the *engrailed (en)* gene from *P. phalangioides* were obtained via nested PCR with degenerated primers as previously described for *Cupiennius salei* (Damen 2002). Additional sequence information was obtained by RACE PCR with the following primers (3′RACE: CGGCGACAGGATTTGGCCCG, 5′ RACE: CGGGCCAAATCCTGTCGCCG). The sequence of *en* from *P. phalangioides* is available from GenBank under the accession number LT160036.

Whole-mount in situ hybridisation and nuclei stainings

Whole mount in situ hybridisation was performed according to the protocol in Prpic et al. (2008b). Riboprobes for the detection of *en* expression were transcribed from the 3′ RACE PCR clone (867 bp) and labelled with digoxygenin (Roche). To visualise the nuclei under UV light, the embryos were treated with SYTOX-Green (Invitrogen) as previously described (Turetzek et al. 2016). Digital images were taken either with white light or with UV light under a Leica M205 FA binocular microscope equipped with a QImaging Micropublisher 5.0 RTV camera. A combination of white and UV light was used to better depict embryo morphology in the specimens stained with blue precipitate resulting from the in situ hybridisation reaction. Correction of colour values and brightness of all digital images was done with Adobe Photoshop CS5 Extended or CS6 for Apple Macintosh.

Live imaging of embryonic development of *P. phalangioides*

For the observation of live embryos under the microscope, the embryos were placed in a glass block dish and entirely covered with Voltalef H10S oil (Arkema) and illuminated with white light from a cold light source. Still images were taken in intervals of 10 min. To obtain time-lapse movies of the embryonic development of *P. phalangioides*, the separate images were then combined into a movie file using iMovie version 10.0.5 (Apple Inc.), so that every image is shown for 0.05 s.

Results

Formation of the germ band in *P. phalangioides*

The first sign of the transformation of the radially symmetric embryonic anlage into the bilaterally symmetric germ band is the aggregation of cells at the centre of the embryonic anlage, thus forming the primary thickening (Fig. 1a). At 25 °C, the primary thickening is visible approximately 48 h after egg deposition (h AED; see Table 1). About 10 h later, a smaller cell mass, the so-called cumulus, separates from the primary thickening and migrates towards the rim of the embryonic anlage (Fig. 1b). During migration, the cumulus initially

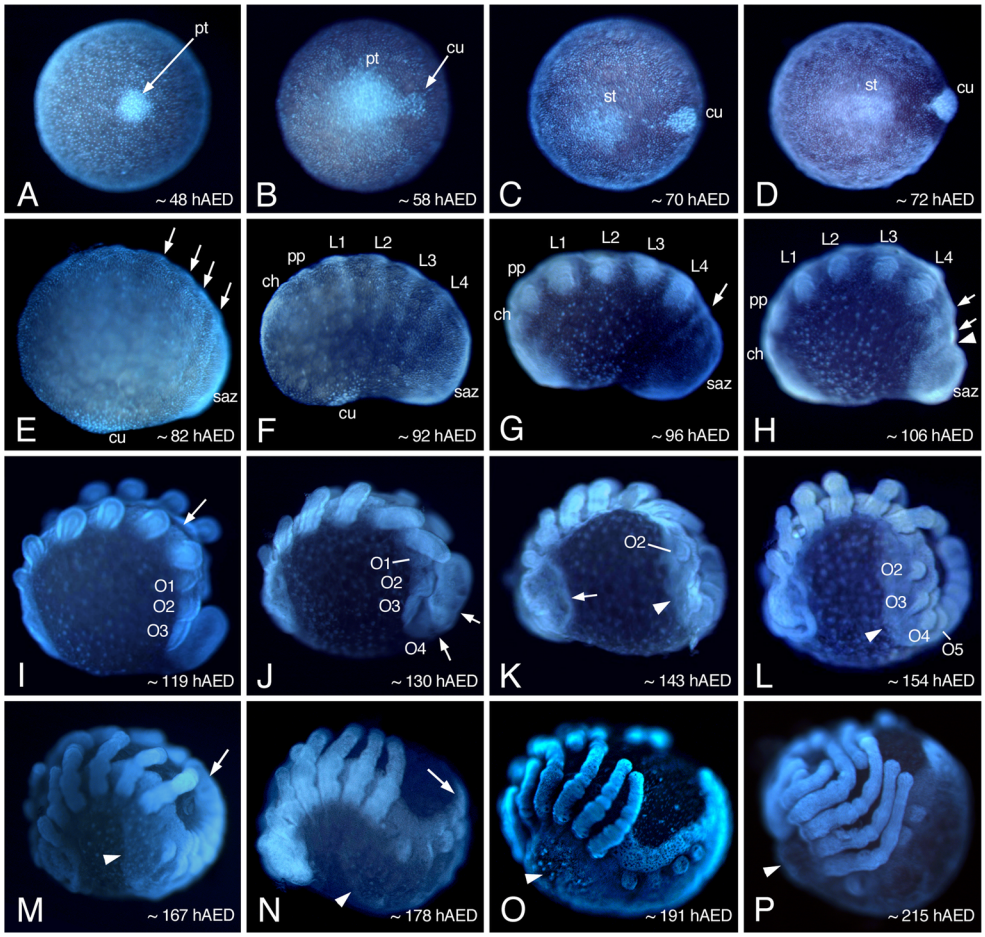

Fig. 1 Consecutive stages of germ band formation and differentiation in *P. phalangioides*. **a** *Top view* of the embryonic anlage with the primary thickening of cells in its centre. **b** Cumulus cells separate from the primary thickening. **c** The cumulus is fully separated and secondary thickening has formed. **d** Cumulus has reached the rim of the embryonic anlage. **e** Pear-shaped germ band has formed; segments are visible in the posterior part (*arrows*). **f** Anterior segments are visible; embryo attains bean-shape. **g** First opisthosomal segment is visible (*arrow*). **h** Segment addition zone bulges outward and prosomal limb buds form. More opisthosomal segments are present (*arrows*) or are in statu nascendi (*arrowhead*). **i** Ventral sulcus forms (*arrow*); tube shaped portion of the opisthosoma elongates. **j** Opisthosomal limb buds appear; segments are visible in the tube shaped portion of the opisthosoma (*arrows*). **k** Brain differentiation begins (*arrow*); dorsal tissue develops on the opisthosomal segments (*arrowhead*). **l** Dorsal tissue grows further (*arrowhead*). **m** Dorsal tissue overgrows the yolk (*arrowhead*); opisthosomal segments are sequentially folded down on the yolk (*arrow*). **n** Dorsal tissue is almost closed (*arrowhead*); most opisthosomal segments are now folded down on the yolk (*arrow*). **o** Dorsal closure complete (*arrowhead*). **p** Prosomal shield forms (*arrowhead*). For further details for each stage, please see text. Embryos in **e**–**p** are shown with anterior to the left and ventral up. *ch* cheliceral segment, *cu* cumulus, *L1–L4* leg segments 1 to 4, *O1–O10* opisthosomal segments 1 to 10, *saz* segment addition zone, *pp* pedipalpal segment, *pt* primary thickening, *st* secondary thickening, *hAED* hours after egg deposition

remains connected with the primary thickening via a thinner stalk of cells. As soon as the cumulus cell mass separates from the primary thickening, the cells of the primary thickening start dispersing across the entire embryonic anlage. This leads to the dissolution of the primary thickening until it is not visible anymore. At approximately 70 h AED, the connection between the dissolving primary thickening and the migrating cumulus disappears, and at the same time, the cells at the centre of the disc appear denser again, thus forming a cell mass similar to the primary thickening but less dense, that we term the secondary thickening (Fig. 1c). At approximately 72 h AED, the cumulus cells have reached the outer part of the embryonic anlage (Fig. 1d). Now, the secondary thickening starts dissolving, and the cells segregate and form a new and enlarged structure, the segment addition zone. This event marks the symmetry break that defines the anterior-posterior axis of the germ band, and the formation of a bilaterally symmetric germ band is completed at approximately 82 h AED, when the germ band shows the first morphological signs of segmentation (Fig. 1e).

Segmentation and further differentiation of the germ band

In the early germ band, the anterior region is poorly defined, but in the posterior half, four segment precursors are visible (Fig. 1e). The embryo now appears pear-shaped because the

Table 1 Timing of developmental events during germ band formation and differentiation in embryos of *P. phalangioides* at 23 °C

48 h AED (Fig. 1A)	Primary thickening forms in the centre of the embryonic anlage
58 h AED (Fig. 1B)	Cumulus migration starts Primary thickening cells disperse
70 h AED (Fig. 1C)	Connection between cumulus and remnant of primary thickening disappears Secondary thickening visible
72 h AED (Fig. 1D)	Cumulus reaches rim of embryonic anlage Cells of the secondary thickening disperse: formation of the segment addition zone Radial symmetry is broken: bilaterally symmetric germ band forms
82 h AED (Fig. 1E)	First segments are visible in the posterior portion
92 h AED (Fig. 1F)	Embryo attains bean-shape All prosomal segments are morphologically visible Cumulus slowly disappears
96 h AED (Fig. 1G)	Prosomal segments well delineated First opisthosomal segment visible Cumulus not visible anymore
106 h AED (Fig. 1H)	Prosomal limb buds formed Segment addition zone bulges outward Three opisthosomal segment anlagen present
119 h AED (Fig. 1I)	Prosomal limbs elongate Tube shaped portion of the opisthosoma forms and elongates Three opisthosomal segments well developed and lying on the yolk Ventral sulcus appears
130 h AED (Fig. 1J)	Limb buds on O2 start forming Segments in tube shaped portion of the opisthosoma clearly delineated Segment O4 opens and folds down on yolk
143 h AED (Fig. 1K)	Brain differentiation begins Dorsal tissue develops on opisthosoma: start of inversion More segments are added posteriorly
154 h AED (Fig. 1L)	Opisthosomal limb buds are well formed Segment O5 opens and folds down on yolk
167 h AED (Fig. 1M)	Mid inversion: dorsal tissue grows Tube shaped portion of opisthosoma shortens by folding down more segments to the yolk
178 h AED (Fig. 1N)	Late inversion: dorsal tissue overgrows yolk Tube shaped portion of opisthosoma shortened; only comprising two segments
191 h AED (Fig. 1O)	Dorsal closure Tube shaped portion of opisthosoma gone; all segments folded down on yolk
215 h AED (Fig. 1P)	Prosomal shield begins differentiating Ventral closure begins
225 h AED	Prosomal shield fully formed; pulls legs apart Ventral prosoma closed
239 h AED	Ventral closure complete Dramatic leg length growth starts
263 h AED	Legs wrap body Eyes are pigmented

Please note that all time points given in the table are approximate values
h AED hours after egg deposition

segment addition zone slightly protrudes and takes up the entire posterior end of the embryo. The cumulus is still visible on the opposite side of the germ band (the future dorsal side, where no dorsal tissue has developed yet) (Fig. 1e), but then gradually disappears (Fig. 1f) until it has completely vanished at around 96 h AED (Fig. 1g). At approximately 92 h AED, the germ band is more differentiated also in the anterior portion and the whole embryo is now bent into a bean-shape (Fig. 1f). The segmental anlagen of the cheliceral, pedipalpal and the four walking legs are morphologically visible, and at the molecular level, a further segmental anlage is already present in the segment addition zone as visualised by the expression of the segment polarity gene *engrailed* (*en*) (arrow, Fig. 2a). At approximately 96 h AED, the prosomal segments are fully delineated and the first opisthosomal segment (O1) is now also morphologically separated from the segment addition zone (Fig. 1g). At this stage, also the differentiation of the prosomal limb buds starts, and slightly later, at around 106 h AED, the buds are formed (Fig. 1h). At this stage, the segment addition zone is strongly bulging outward (Fig. 1h), and the segments it generates over the following stages therefore grow away from the embryo and form a tube-shaped structure that points into the perivitelline space (Fig. 1i–l) (see also next chapter for a detailed description of this mode of opisthosoma development). All segments, including those in the tube shaped portion, express the segment polarity gene *engrailed* in their posterior part (Fig. 2b–d). The prosomal appendages continue growing (Fig. 1i), and at approximately 130 h AED, also the limb buds on the second opisthosomal segment (O2) are specified (Fig. 1j, k) and later also the limb buds on the third to fifth opisthosomal segment (O3-O5) are visible (Fig. 1l). At approximately 143 h AED, the head lobes enlarge indicating the beginning morphological differentiation of the brain (Fig. 1k).

Development of the opisthosoma

A feature of germ band development of *P. phalangioides*, which differs from the entelegyne spiders observed so far, is the mode of opisthosoma formation. The first three opisthosomal segments are generated by the segment addition zone, while it is still closely attached to the yolk (Fig. 3a, b). These three segments are therefore lying on the yolk in the same way as the more anterior segments (Fig. 3b). Then, the segment addition zone starts bulging outwards causing all further segments to be oriented away from the egg, eventually forming a tube-shaped structure (Fig. 3c–e). The posterior segments in this portion of the opisthosoma are closed, but like the more anterior segments do not have any true dorsal tissue yet. This is revealed by a detailed sequence of segment formation in the opisthosoma (Fig. 4). Opisthosomal segment 4 (O4) is the first opisthosomal segment that is formed with an orientation away from the egg (see Fig. 3c, d). However, during further development, it opens on its back and the two halves are then folded down on the yolk. Now, the O4

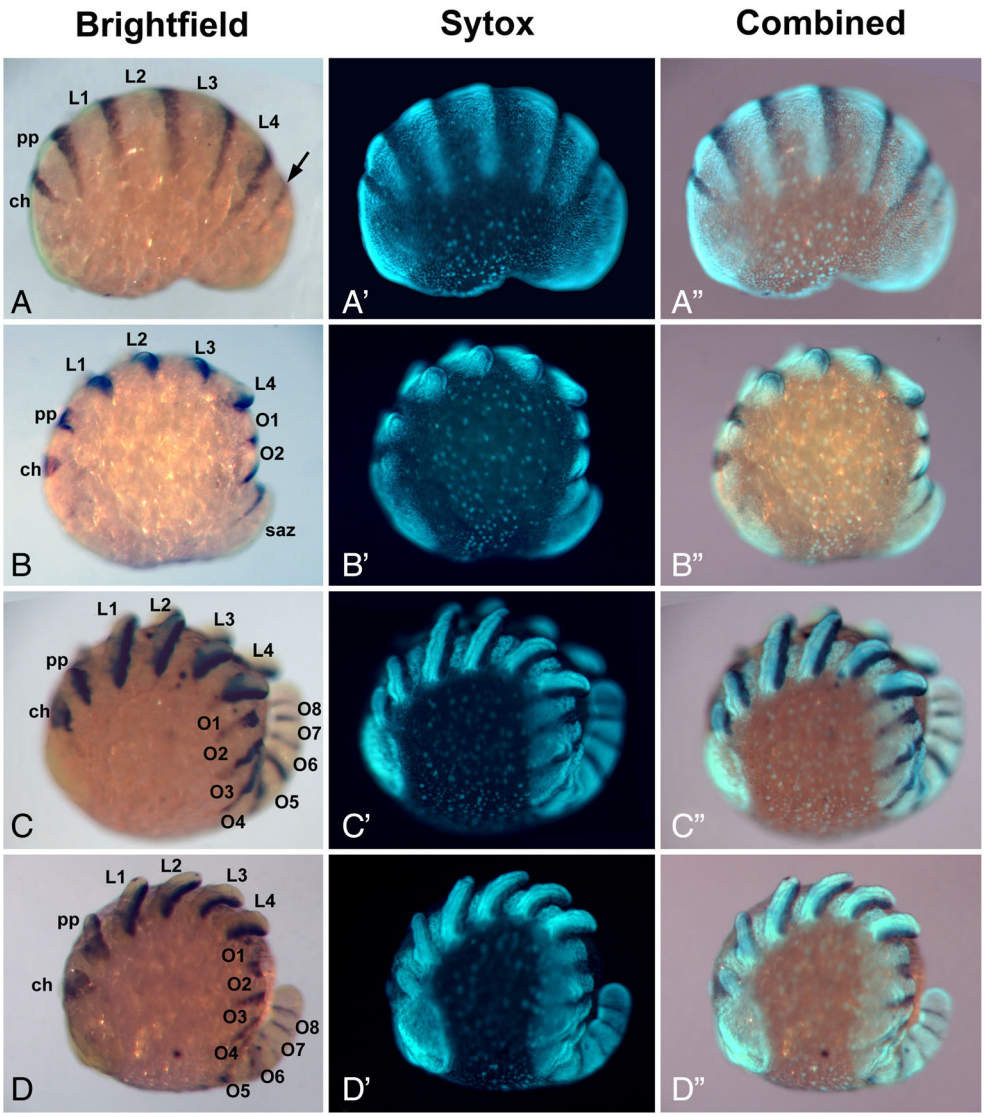

Fig. 2 Expression of *engrailed* (*en*) in the germ band of *P. phalangioides*. **a** Embryo at the bean-shaped stage. All prosomal segments are visible and express *en* in their posterior portion. Expression of *en* also prefigures the first opisthosomal segment formed by the segment addition zone (*arrow*). **b** The segment addition zone bulges outward and further opisthosomal segments are formed, all denoted by *en* expression. **c**, **d** Segments in the tube shaped portion of the opisthosoma also express *en*. **a′**–**d′** The same embryos as in **a**–**d**, respectively, cell nuclei have been stained with Sytox Green and visualised with UV light. **a″**–**d″** The same embryos as in **a**–**d**, respectively. Combined detection of cell nuclei (UV light) and gene expression (white light). All embryos are shown with anterior to the left and ventral up. See abbreviations in Fig. 1

segment is very similar to the segments O1 to O3 (Fig. 4a). In particular, like the segments O1 to O3, the O4 segment also has no proper dorsal tissue yet; this tissue forms afterwards during the later phases of inversion (see below). The segment addition zone continuously adds segments to the opisthosoma (Fig. 4b) whereby the tube shape portion initially becomes longer. But, at the same time, more segments are opened "dorsally" and folded down on the yolk (Fig. 4c, d). In this way, the tube shaped portion of the opisthosoma becomes shorter after the segment addition zone has generated the O10 segment and has terminated its activity (Fig. 4d, e). Finally, all opisthosomal segments are folded down on the yolk (Fig. 4f).

Inversion and dorsal closure

As a preparation for inversion, the germ band starts splitting along the ventral midline at approximately 119 h AED (Fig. 1i). This formation of the ventral sulcus initiates the ventral opening necessary for inversion, but on the dorsal side, no inversion-specific events occur before approximately 143 h AED when genuine dorsal tissue develops on the opisthosomal segments (Fig. 1k, arrow and arrowhead). This dorsal tissue overgrows the yolk during the following stages (Fig. 1k–n, arrowheads) until the two leading edges meet and fuse on the dorsal side during dorsal closure (Fig. 1o, arrowhead). After the dorsal side of the prosoma has closed over the yolk, there is further differentiation of this tissue when it further contracts and forms the uniform prosomal shield (Fig. 1p) at approximately 215 h AED. At this stage, all opisthosomal segments have been folded down on the yolk. Although this process also leads to a partial closure of the ventral side of the embryo (Fig. 5a, b), the ventral side is still open at the time when the dorsal side is fully closed and the prosomal shield has formed (Fig. 5c). However, ventral closure proceeds quickly and the prosoma is closed first (Fig. 5d), and shortly after, the ventral side is closed entirely (Fig. 5e).

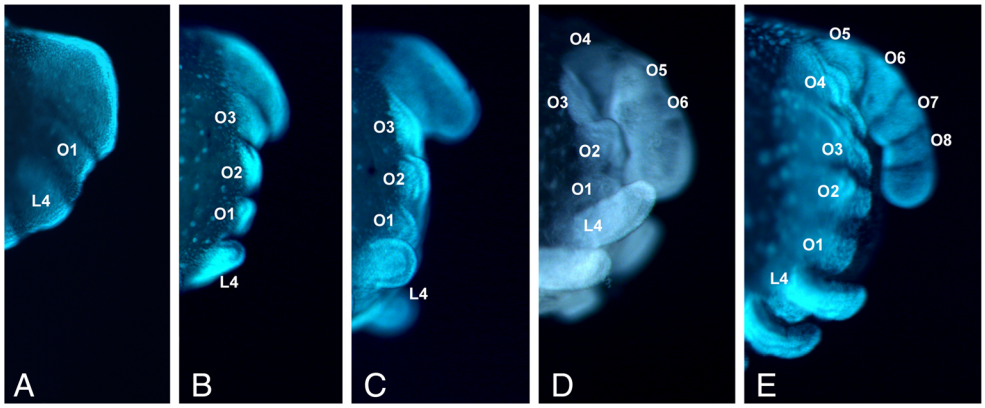

Fig. 3 Formation of the tube shaped portion of the opisthosoma. **a** The segment addition zone starts bulging outward after it has initiated the formation of the O1 segment. **b**, **c** After the formation of the segments O1 to O3, the segment addition zone orients away from the body (**b**) and elongates (**c**). **d**–**e** All following segments are then formed away from the yolk in a tube shaped structure (**d**) that therefore elongates (**e**) before it shortens again, because the more anterior segments (i.e., more proximal in the tube shaped portion) are successively folded down on the yolk (see Fig. 4). See abbreviations in Fig. 1

Growth of the legs

Because of the extremely long legs in adult *P. phalangioides*, we also studied the development of the walking legs during embryogenesis. The legs first appear as small limb buds at approximately 106 h AED (Fig. 1h). During inversion, the prosomal appendages further elongate (Fig. 1k–n) and differentiate during dorsal closure so that the podomeres of the walking legs become morphologically visible (Fig. 1m). Despite its long legs in the adult animal, the legs of *P. phalangioides* are not extraordinarily long before dorsal closure is completed (Fig. 5a). However, with the start of the ventral closure, the legs have grown considerably and now especially the distal portion of the first leg pair is overlapping, thus giving the impression that the legs are "too long" to fit next to each other and the embryo looks like "folding its arms" (Fig. 5b). This impression is lost again when the dorsal side compacts during the formation of the prosomal shield (Fig. 5c) and this contraction of the

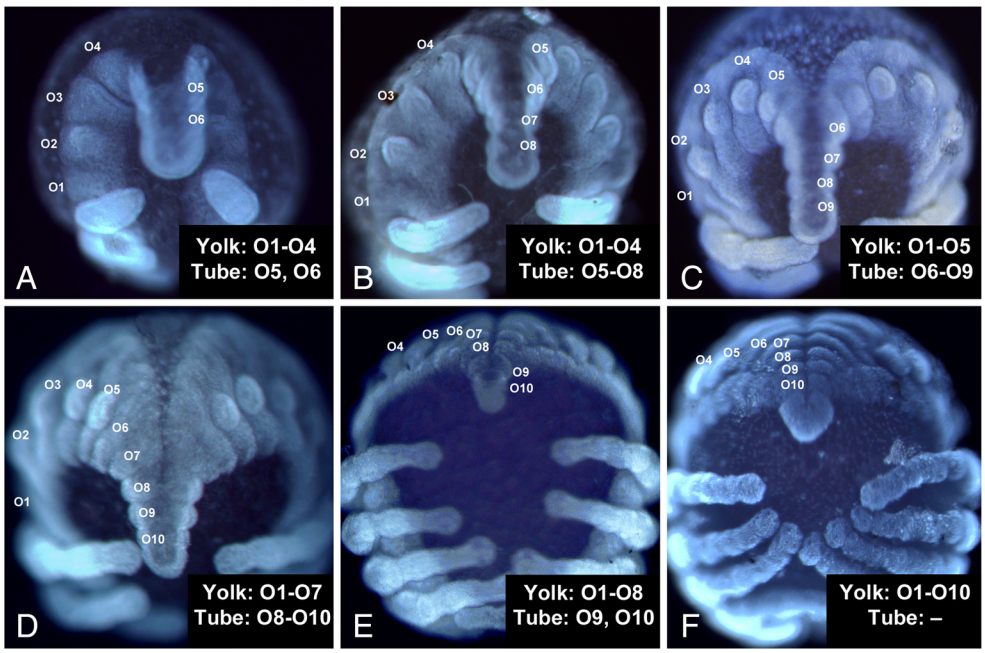

Fig. 4 Formation of the opisthosoma by folding down segments on the yolk. **a**–**b** The number of segments in the tube-shaped portion of the opisthosoma grows continuously, but the O4 segment is already at the "hinge" between the segments on the yolk and segments in the tube (**a**) or fully folded down on the yolk (**b**). **c**–**e** The segment addition zone produces more segments, but the speed of folding down segments also increases, thus leading to a shortening of the tube-shaped portion. **f** Because the segment addition zone stops producing segments at one point, but the folding down of segments continues, all segments are eventually folded down on the yolk. The number of segments already lying on the yolk ("yolk") and those still in the tube shaped portion of the opisthosoma ("tube") is given in each panel at the lower right corner. See abbreviations in Fig. 1

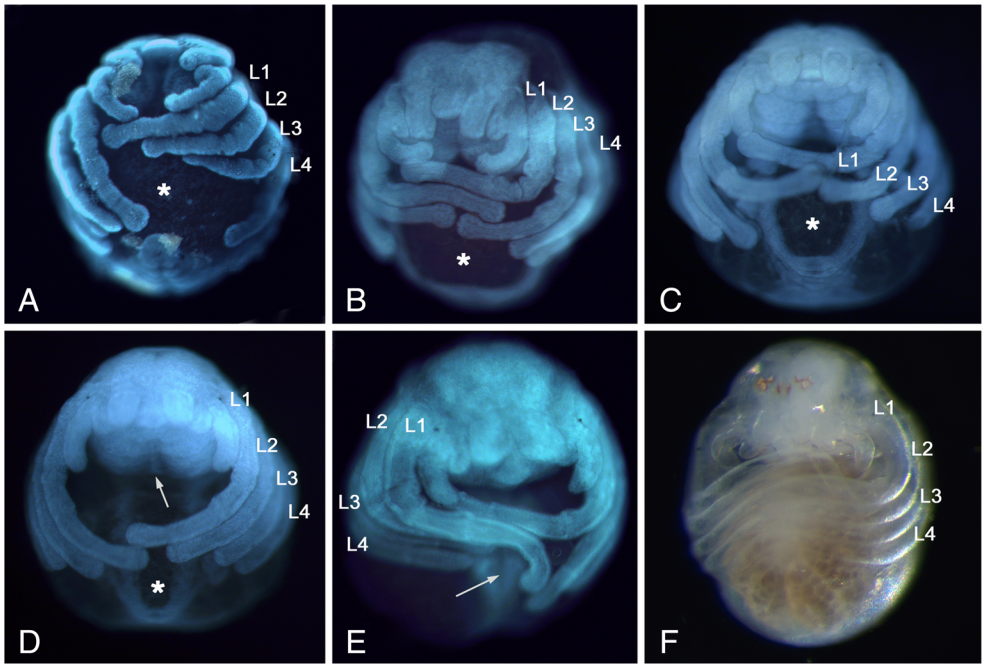

Fig. 5 Allometric growth of the legs in *P. phalangioides*, and ventral closure. **a** Shortly before dorsal closure, the legs are moderately long and the ventral side is still wide open (*asterisk*). **b** When the dorsal side is closed, the legs (especially the first leg pair) interlace. Ventral closure has started, and the gap between left and right half is closing (*asterisk*). **c**, **d** The formation of the prosomal shield on the dorsal side pulls apart the interlaced legs. Ventral closure proceeds (*asterisk*) and is first complete in the prosoma (*arrow* in **d**). **e**, **f** When ventral closure is complete (*arrow* in **e**), a sudden increase in leg growth occurs, and in stages shortly before hatching, the legs are fully wrapped around the body (**f**). See abbreviations in Fig. 1

dorsal side also pulls apart the entangled legs (Fig. 5d). Coinciding with complete ventral closure, there is a sudden increase in leg growth that leads to the legs overlapping again and the tips are often twisted, obviously because there is not enough space now to accommodate the long legs (Fig. 5e). This length growth continues throughout the rest of embryonic development, and in embryos shortly before hatching, the legs are so long that they are wrapped around the body (Fig. 5f; Supplementary Information, Movie S2). Our data show that leg development in *P. phalangioides* is initiated during the early phases of germ band elongation similar to previous studies in entelegyne spiders with shorter legs (e.g., Mittmann and Wolff 2012; Wolff and Hilbrant 2011) and that leg length growth during inversion also does not differ significantly from these species. A significant increase in leg length is then seen after dorsal closure (Supplementary Information, Movie S2), and a similar phase of increased length growth has not been reported from other species with shorter legs.

Discussion

Primary and secondary thickening

The formation of a primary thickening and the migration of the cumulus are features common to all spiders and have previously been described for *P. phalangioides* as well (Claparède 1862; Emerton 1872). However, our observations provide evidence that after the primary thickening has disappeared, a second thickening appears at the centre of the disc shaped embryonic anlage. The formation and disappearance of the primary thickening involves the migration of cells towards the disc centre and then their dispersal all across the embryonic anlage. The formation of the secondary thickening is less clear. It appears after most of the former primary thickening cells have already dispersed. Our time-lapse recording of this process (Supplementary Information, Movie S1) suggests that at least a part of the secondary thickening is formed by former primary thickening cells that reverse their movement and come together a second time at the centre of the embryonic anlage. However, we cannot exclude the possibility that local cell division and cell shape changes also contribute to the emergence of the secondary thickening.

Our results show that the segment addition zone is formed from the secondary thickening by expanding its area. The migrating cumulus ends up at a position in the extraembryonic area of the egg and then disappears. Note, however, that Edgar et al. (2015) have recently devised a new model of spider development that proposes that the cells of the migrating cumulus also end up in the segment addition zone. This model is

based on studies of germ band formation in the entelegyne species *Latrodectus mactans*, *Latrodectus geometricus*, and *Cheiracanthium mildei* but is not compatible with the results from *Parasteatoda tepidariorum* (Akiyama-Oda and Oda 2003) and *P. phalangioides* (this study). Further studies are necessary to clarify the mechanisms of these early cell rearrangements and cell movements and their function and importance for the development of the germ band.

Comparisons with previous spider embryonic staging charts

A detailed developmental embryonic staging has been published previously for the entelegyne spiders *Cupiennius salei* (Wolff and Hilbrant 2011) and *Parasteatoda tepidariorum* (Mittmann and Wolff 2012). These staging charts agree well for the early phases of embryonic development but differ for later embryonic stages. Whereas the formation of the blastoderm and the processes that result in the bilaterally symmetric germ band (i.e., formation of the embryonic anlage, cumulus formation and migration) have been subdivided into 7 consecutive stages in both species, the later developmental processes concerning further morphological differentiation of the germ band until hatching are in contrast subdivided into 14 stages in *C. salei*, and 7 stages in *P. tepidariorum*. It is therefore difficult to directly align and compare the staging charts of the two species, which also precludes a direct comparison with the developmental processes documented in the present work of the haplogyne spider *P. phalangioides*. In general, however, early development until the formation of the germ band (stage 7 in *P. tepidariorum* and *C. salei*) is more uniform in the three species, whereas later development is more diverse including specific processes not present in all species. In particular, in *P. phalangioides*, the bulging of the segment addition zone that coincides with the appearance of the prosomal limb buds (i.e., stage 9 in *C. salei* and stage 8 in *P. tepidariorum*) is preceded by a peculiar bending of the entire embryo resulting in a "bean-shape"-stage that is not present in the developmental chart of either *C. salei* or *P. tepidariorum*. In addition, the onset of a second phase of length growth of the walking legs in *P. phalangioides* that coincides with the beginning of ventral closure (stage 20 in *C. salei* and stage 14 in *P. tepidariorum*) is present only in *P. phalangioides*. The time required for the entire development from the first cleavage to ventral closure differs quite substantially between the three species and also appears to be correlated with body size of the adult spiders. The largest species, *C. salei*, requires ca. 280 h to complete ventral closure (Wolff and Hilbrant 2011), whereas the smallest species, *P. tepidariorum*, has completed ventral closure at ca. 180 h (Mittmann and Wolff 2012). *P. phalangioides* is intermediate both in body size and in terms of developmental time; it requires ca. 240 h to complete ventral closure.

"Preabdomen-postabdomen" subdivision of the opisthosoma

Most studies of spider germ band development have focused on entelegyne spiders, and this also includes most recent models for developmental genetic studies (e.g., Abzhanov and Kaufman 2000; Akiyama-Oda and Oda 2003; McGregor et al. 2008). In these spiders, the opisthosoma develops from a segment addition zone that remains attached to the yolk surface throughout development. Therefore, all opisthosomal segments that are formed by the segment addition zone lie on the yolk surface as well, and the opisthosoma gradually grows around the yolk as segmentation proceeds. By contrast, in *P. phalangioides*, the formation of the opisthosoma is a two-phase process: The first three segments are formed like in entelegyne spiders, but then, the segment addition zone bulges away from the body and therefore produces the remaining segments in a tube-shaped structure. Intriguingly, this developmental mode has been reported not only from *P. phalangioides* (Claparède 1862; Emerton 1872) but also from several other haplogyne spiders (Holm 1940), and also from Mygalomorphae (bird spiders) (Yoshikura 1958; Crome 1963;

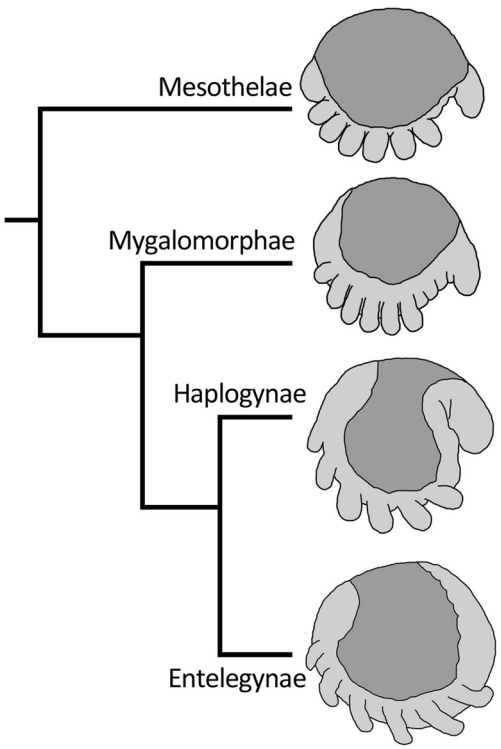

Fig. 6 Spider phylogeny and developmental modes of the opisthosoma. The basally branching taxa *Mesothelae* and *Mygalomorphae*, and the *Haplogynae* show a mode of opisthosoma development that involves the formation of a tube-shaped portion. In the *Entelegynae*, all opisthosomal segments are lying on the yolk and no tube-shaped portion is formed. The phylogeny of the spider taxa is simplified after Bond et al. (2014). The embryo drawings are shown with anterior to the left and ventral down and have been redrawn after Yoshikura (1954) (Mesothelae), Yoshikura (1958) (Mygalomorphae), Holm (1940) (Haplogynae), and Holm (1952) (Entelegynae)

Crome 1964), and even from the Mesothelae (segmented spiders), the most basally-branching spider group (Yoshikura 1954). Thus, although this mode is unusual when compared to other chelicerates and other arthropods, it appears to be the primitive mode of posterior segment addition in spiders (see summary in Fig. 6).

Holm (1940) has coined the terms "preabdomen" and "postabdomen" for those segments on the yolk and those segments in the tube-shaped portion of the opisthosoma, respectively. He suggested that these two parts of the opisthosoma in non-entelegyne spiders are a remnant of a phylogenetically older subdivision of the arachnid opisthosoma into two subtagmata, and he compares the spider "pre-" and "postabdomen" to the mesosoma and metasoma of scorpions. Our data do not support this notion, because the initial border between "preabdomen" and "postabdomen" as defined by Holm (1940) is between the third and the fourth opisthosomal segment, and this border does not correspond to the subdivision of the scorpion opisthosoma. In addition, the border between "preabdomen" and "postabdomen" shifts during development (see Fig. 4) thus making a clear distinction of the two parts anyway difficult. Although Holm's idea of a phylogenetically ancient subdivision of the opisthosoma into "pre-" and "postabdomen" is therefore not supported by the currently available data, we note, however, that an opisthosomal subborder between the third and fourth opisthosomal segment is actually present in adult Ricinulei (hooded tickspiders) (Weygoldt 1996). Unfortunately, to the best of our knowledge, nothing is known yet about the embryonic development of Ricinulei, and therefore, it is presently unclear whether the adult subdivision of their opisthosoma corresponds to the same subdivision in their embryos.

The developmental mode of the opisthosoma in basally branching spiders and haplogyne spiders might be related to the development of the pleon in decapod crustaceans. In these crustaceans, the embryonic pleon is also subdivided into a portion that lies flat on the yolk and a portion that grows away from it (so-called caudal papilla) (Sandeman and Sandeman 1991; Scholtz 1992). The portion of the pleon that is formed by the caudal papilla is indeed similar to the tube-shaped portion of the opisthosoma, but it is currently unclear whether these similarities are only superficial, or if there are also developmental or molecular similarities between the two developing structures.

Acknowledgments We thank Matthias Pechmann for advice on cloning the *engrailed* gene from *Pholcus phalangioides* and Maarten Hilbrant for comments on the manuscript. We also thank two anonymous reviewers for valuable comments that significantly improved the manuscript. This work was supported by the Deutsche Forschungsgemeinschaft (grant numbers PR 1109/4-1 and PR 1109/6-1 to N.M.P.). Additional financial backing has been received from the Göttingen Graduate School for Neurosciences, Biophysics and Molecular Biosciences (GGNB), the Göttingen Center for Molecular Biosciences (GZMB), and the University of Göttingen (GAU). N.T. is supported by a Christiane-Nüsslein-Volhard-Foundation fellowship and a "Women in Science" Award by L'Oréal Deutschland and the Deutsche UNESCO-Kommission. The funders had no role in study design, data collection and analysis, decision to publish, or preparation of the manuscript.

Compliance with ethical standards

Competing interests N.M.P. is a member of the Editorial Board of Development Genes and Evolution serving as Communicating Editor for the Topical Collection "Size & Shape".

References

Abzhanov A, Kaufman TC (2000) Homologs of *Drosophila* appendage genes in the patterning of arthropod limbs. Dev Biol 227:673–689

Akiyama-Oda Y, Oda H (2003) Early patterning of the spider embryo: a cluster of mesenchymal cells at the cumulus produces dpp signals received by germ disc epithelial cells. Development 130:1735–1747

Akiyama-Oda Y, Oda H (2006) Axis specification in the spider embryo: *dpp* is required for radial-to-axial symmetry transformation and sog for ventral patterning. Development 133:2347–2357

Akiyama-Oda Y, Oda H (2010) Cell migration that orients the dorsoventral axis is coordinated with anteroposterior patterning mediated by hedgehog signaling in the early spider embryo. Development 137: 1263–1273

Bond JE, Garrison NL, Hamilton CA, Godwin RL, Hedin M, Agnarsson I (2014) Phylogenomics resolves a spider backbone phylogeny and rejects a prevailing paradigm for orb web evolution. Curr Biol 24: 1765–1771

Claparède É (1862) Recherches sur l'évolution des araignées. Natuurkundige Verhandelingen uuitgegeven door het Provinciaal Utrechtsch Genootschap von Kunsten en Wetenschappen. Deel I, Stuk 1. C van der Post Jr, Utrecht

Crome W (1963) Embryonalentwicklung ohne "Umrollung" (=Reversion) bei Vogelspinnen (Araneae: Orthognatha). Deutsche Entomologische Zeitschrift Neue Folge 10:83–95

Crome W (1964) Eikokon, Embryonalstadien und frühe Jugendformen von *Conothele arboricola* Pocock (Araneae: Ctenizidae). Zoologische Jahrbücher Abteilung für Systematik, Ökologie und Geographie der Tiere 91:411–450

Damen WGM (2002) Parasegmental organization of the spider embryo implies that the parasegment is an evolutionary conserved entity in arthropod embryogenesis. Development 129:1239–1250

Edgar A, Bates C, Larkin K, Black S (2015) Gastrulation occurs in multiple phases at two distinct sites in *Latrodectus* and *Cheiracanthium* spiders. EvoDevo 6:33

Emerton JH (1872) Observations on the development of *Pholcus*. Proc Boston Soc Nat Hist 14:393–395 Plate II

Holm Å (1940) Studien über die Entwicklung und Entwicklungsbiologie der Spinnen. Zoologiska Bidrag från Uppsala 19:1–214 Plates 1-11

Holm Å (1952) Experimentelle Untersuchungen über die Entwicklung und Entwicklungsphysiologie des Spinnenembryos. Zoologiska Bidrag från Uppsala 29:293–424 Plates 1-6

Huber BA (2011) Revision and cladistic analysis of *Pholcus* and closely related taxa (Araneae, Pholcidae). Bonner Zoologische Monographien 58:1–509

McGregor AP, Hilbrant M, Pechmann M, Schwager EE, Prpic NM, Damen WG (2008) *Cupiennius salei* And *Achaearanea tepidariorum*: spider models for investigating evolution and development. BioEssays 30:487–498

Mittmann B, Wolff C (2012) Embryonic development and staging of the cobweb spider *Parasteatoda tepidariorum* C. L. Koch, 1841 (syn.: *Achaearanea tepidariorum*; Araneomorphae; Theridiidae). Dev Genes Evol 222:189–216

Pechmann M, Khadjeh S, Turetzek N, McGregor AP, Damen WG, Prpic NM (2011) Novel function of *Distal-less* as a gap gene during spider segmentation. PLoS Genet 7:e1002342

Prpic NM, Schoppmeier M, Damen WGM (2008a) Collection and fixation of spider embryos. Cold Spring Harbor Protoc 3:930–932. doi:10.1101/pdb.prot5067

Prpic NM, Schoppmeier M, Damen WGM (2008b) Whole-mount in situ hybridization of spider embryos. Cold Spring Harbor Protoc 3:933–936. doi:10.1101/pdb.prot5068

Sandeman R, Sandeman D (1991) Stages in the development of the embryo of the fresh-water crayfish *Cherax destructor*. Roux's arch. Dev Biol 200:27–37

Scholtz G (1992) Cell lineage studies in the crayfish *Cherax destructor* (Crustacea, Decapoda): germ band formation, segmentation, and early neurogenesis. Roux's arch. Dev Biol 202:36–48

Turetzek N, Pechmann M, Schomburg C, Schneider J, Prpic NM (2016) Neofunctionalization of a duplicate *dachshund* gene underlies the evolution of a novel leg segment in arachnids. Mol Biol Evol 33: 109–121

Weygoldt P (1996) Chelicerata, Spinnentiere. In: Westheide W, Rieger R (eds) Spezielle Zoologie. Teil 1: Einzeller und Wirbellose Tiere. Gustav Fischer Verlag, Stuttgart, pp. 449–497

Wolff C, Hilbrant M (2011) The embryonic development of the central American wandering spider *Cupiennius salei*. Front Zool 8:15

Yoshikura M (1954) Embryological studies on the liphistiid spider *Heptathela kimurai*, part I. Kumamoto J Sci Ser B (Biology and Geology) 3:41–48 Plate I

Yoshikura M (1958) On the development of a purse-web spider, *Atypus karschi* Dönitz. Kumamoto J Sci Ser B Sect 2 Biol 3(2):73–86